NeuroImage 62 (2012) 1884–1895

Contents lists available at SciVerse ScienceDirect

NeuroImage

journal homepage: www.elsevier.com/locate/ynimg

Cortical dynamics of human scalp EEG origins in a visually guided motor execution ☆

Hiroaki Mizuhara *

Graduate School of Informatics, Kyoto University, Yoshida-Honmachi, Sakyo-ku, Kyoto 606-8501, Japan

ARTICLE INFO

Article history:
Accepted 27 May 2012
Available online 31 May 2012

Keywords:
Mu rhythm
Alpha rhythm
Gamma rhythm
Simultaneous fMRI and EEG
Source estimation

ABSTRACT

The EEG mu rhythm is often used as an index of activation in the sensorimotor cortex. However, the blur caused by volume conduction makes it difficult to identify the exact origin of the EEG rhythm in the brain using only the human scalp EEG. In this study, simultaneous fMRI and EEG measurements were performed during a visually guided motor execution task in order to investigate whether the mu rhythm in the scalp EEG is an indication of the activity in the sensorimotor cortex. In addition, a new method was proposed for reconstruction of the cortical EEG activity through the fusion of fMRI and EEG data. A suppression of mu rhythm appeared around the lateral central electrode sites, just above the sensorimotor cortex, in association with the activity in that region. During a visually guided motor execution task, the alpha rhythms at the occipital electrode sites and the alpha rhythm at the central electrode sites also showed a correlation with the fMRI signal in the occipital and the supplementary motor cortices, respectively. This method allows the investigation of the scalp EEG origin with the spatial precision of fMRI, while retaining dynamic properties of the cortex with the temporal precision of EEG.

© 2012 Elsevier Inc. All rights reserved.

Introduction

Electroencephalography (EEG) has been widely used to investigate the human brain since Hans Berger made the first human EEG recording in the middle of 1920s (Millett, 2001). The EEG has a particular advantage in that its temporal resolution with millisecond precision allows the investigation of details of the dynamics of cognitive function. It also has the advantage that the scalp EEG is a non-invasive, non-surgical method for recording neuronal activity. These advantages have led many researchers to use scalp EEGs for in-depth exploration of brain function and for development of non-invasive brain machine/computer interfaces.

Recently, much attention has been devoted to the 'mu' EEG rhythm, which has a central frequency almost same as the alpha activity (8–12 Hz). The mu rhythm is often observed during motor execution or motor imagery at the lateral central electrode sites on the scalp, which corresponds to a location just above the sensorimotor cortex (Pfurtscheller et al., 1997; Tiihonen et al., 1989; Wolpaw et al., 2002). Intracranial EEG recordings also localize the mu rhythm around the sensorimotor cortex (Miller et al., 2007; Pfurtscheller et al., 2003). Therefore, this rhythm is often used to indicate activation of the sensorimotor cortex in studies on the mirror neuron system and on brain computer interfaces, etc. (Dumas et al., 2010; Orgs et al., 2008; Ulloa and Pineda, 2007).

However, the scalp EEG is a spatially blurred signal because volume conduction in the EEG measurements interferes with the identification of the origin of the scalp EEG. The scalp EEG is the sum of multiple neuronal activities in the cortices. These neuronal activities occur in the sensorimotor cortex and also in other cortices, so the mu rhythm observed in a scalp EEG may be contaminated by activities from other cortical areas. Therefore, identifying the exact origin of the mu rhythm is difficult using only a human scalp EEG.

This limitation has been overcome in a number of previous studies through the use of simultaneous recordings of functional magnetic resonance imaging (fMRI) and EEG. These studies identified the origin of the scalp EEG using an EEG power time series as the predictor or explanatory variable for simultaneously recorded fMRI signals (Kiebel and Friston, 2004; Valdes-Sosa et al., 2009). Thus, a direct comparison of the temporal fluctuation of the EEG and fMRI can be used to identify the EEG origin with the spatial precision of fMRI. This temporal integration of the fMRI and EEG data has been widely adopted for simultaneous recording of fMRI and EEG data (Kiebel and Friston, 2004; Martinez-Montes et al., 2004; Mizuhara and Yamaguchi, 2007; Mizuhara et al., 2004, 2005).

However, this approach occasionally will falsely indentify activations in other cortices that are also correlated with temporal fluctuations occurring in the true origin. For instance, multiple cortical activities are inter-correlated to the temporal fluctuation of true EEG origin (Fig. 1A); that is, the functional connectivity network in the cerebral cortex. In this situation, a scalp EEG power time series has a temporal correlation to the true origin, but also to other cortical areas that have temporal correlation to the origin. The true EEG origin may be an activity that is occurring just below the electrode used for the

☆ Competing interests: The author declare that no competing interests exist.

* Fax: +81 75 753 3147.
E-mail address: hmizu@i.kyoto-u.ac.jp.

1053-8119/$ – see front matter © 2012 Elsevier Inc. All rights reserved.
doi:10.1016/j.neuroimage.2012.05.072

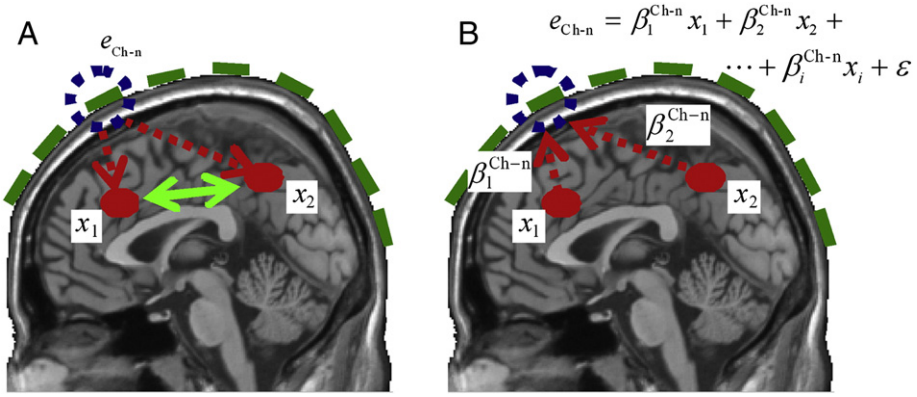

Fig. 1. Comparison of the conventional and the proposed method for binding simultaneously measures fMRI and EEG. (A) The conventional method. The scalp EEG time series values were used as the predictor variables to identify the cortical activity that was correlated with the BOLD temporal fluctuation in the regression analysis. When the scalp EEG ($e_{\text{Ch}-n}$) origin x_1 has the correlation to a region x_2, this method could identify the origin x_1 as well as the correlated region x_2. (B) The proposed method based on the spatial relationship between the cortical activities and scalp EEG. The forward model for estimating the filter coefficient for the beamformer method, where x represents the time series of the cortical activity, $e_{\text{Ch}-n}$ represents the EEG power time series at nth electrode, and β represents the regression coefficient. The red circle represents the cortical activities and the green bars on the scalp represent EEG electrodes.

analysis, but the possibility remains that any of the other cortical areas is also the generator, even though the spatial location of the activity is far from the electrode.

A second approach for the integration of the fMRI and EEG data is to use spatial information in fMRI activation profiles as spatial constraints on EEG origins (Kiebel and Friston, 2004). In this case, the temporal information in the fMRI is usually discounted when constructing the spatial priors (Kiebel and Friston, 2004). The current study has used simultaneous fMRI and EEG measurements as a new method for identifying the origin of scalp EEG. Here, the cortical activities are used as the explanatory variables for multiple regression analysis and to identify the EEG distribution on the scalp, where the blood oxygenation level dependent (BOLD) responses are used as representative signals of the cortical activities (Fig. 1B). The fMRI is used to identify the spatial location of cortices for the analysis and for comparing the temporal fluctuation of EEG signals. This approach could simultaneously satisfy integration through temporal predictions and through spatial constraints. It also used multiple regression analysis with cortical activities as the predictor variables, thereby reducing the risk of contamination from other cortices (the so-called third-party effect), and identifying the true origin of the scalp EEG. It allowed depiction of the spatio-temporal profile of cortical neuronal activities during a visually guided motor execution task.

Materials and methods

Participants and task procedure

Fifteen healthy males, aged 20 to 31 years old (mean ± s.d.: 25.6 ± 3.9 years old) and all right-handed (Edinburgh handedness test, mean ± s.d.: 96.0 ± 8.3), participated in the experiments. One participant was excluded from further analysis due to excessive artifacts in the EEG data. The experimental procedure was approved by the ethics committee at Graduate School of Medicine and Faculty of Medicine, Kyoto University (# E311). Participants gave their written informed consent according to the declaration of Helsinki and were paid for their participation to the study.

The task was a left/right hand grasping task performed in accordance with a visually presented GO signal (white filled circle) presented for 1 s at the right or left hemifield on a black screen. The participants were asked to grasp their hands as quickly and accurately as possible upon the appearance of the visual GO signal. Prior to the signal appearance, an informative cue (white drilled square) was presented. The GO signal stimulus was always presented in the same hemifield with respect to the location of informative cue. The interval between the informative cue and GO signal was set at 1.0, 1.5, or 2.0 s. The inter-stimulus interval was set at 1, 2, or 3 s. The presentation order of the left/right GO signal and the intervals were pseudo-randomized. The GO signal for left/right hand grasping appeared at almost the same frequency. A white fixation cross was always presented at the center of screen during the experiment. Participants completed the 4 min session 5 times while in the MRI scanner.

Simultaneous fMRI and EEG measurements

Two MR compatible amplifiers (Brain Vision MR, Brain Products, Germany) were used to acquire the EEGs during fMRI measurements using a 10% standard system electrode cap with sintered Ag/AgCl ring electrodes (Brain Cap, Falk Minow Services, Germany). The electrodes had 62 EEG channels, one electrocardiogram (ECG) channel, and one electrooculogram (EOG) channel. An FCz electrode, located between Fz and Cz, was used as the measurement reference, while an electrode on the inion was used as the measurement ground. The ECG electrode was set at the back and the EOG electrode was set below the eye at the face. The Brain Vision Recorder (Brain Products, Germany) was used to sample the raw EEG at 5 kHz with a 1-Hz high pass software filter and a 250-Hz low pass hardware filter. Blood oxygenation sensitive echoplanar images (EPI), obtained using a 1.5-Tesla MR scanner (Magnex Eclipse, Shimadzu-Marconi), were obtained simultaneously with the scalp EEG measurements. The fMRI measurement conditions were as follows: repetition time = 3 s, echo time = 49 ms, acquisition time = 2.97 s, flip angle = 90°, field of view = 192 mm, in-plane resolution = 64 × 64, 30 axial slices, and slice thickness = 5 mm without gap (interleaved slice order). The participant's head was immobilized with a vacuum pillow during the measurements.

fMRI analyses for grasping related ROIs

SPM5 software (Wellcome Department of Cognitive Neurology, London, UK, URL: www.fil.ion.ucl.ac.uk/spm) was used for image preprocessing and voxel-based statistical analysis for fMRI data. The first 3 volumes were discarded and slice timing was corrected with respect to the middle slice to remove the time delay of scanning the entire brain. The remaining EPIs (77 volumes for each session × 5 sessions) were transferred into the first image volume for each participant to correct for head motion. The individual EPIs were normalized to a standard brain by applying the parameters estimated by matching the T1 anatomical image to the stereotactic coordinate image from the Montreal Neurological Institute. The EPIs were then smoothed with a 10-mm full-width half-maximum Gaussian kernel.

The voxel-based statistical analysis on the preprocessed EPIs used a general linear model. The presentation of the left/right informative cue stimulus was modeled as the onset of two box-car functions for hand grasping. The duration was defined as the time between onset of the informative cue and the termination of the GO signal. The box-car functions were convolved with the canonical hemodynamic response function, and then used as the regressors for the regression analysis. The six head motion parameters, derived from the realignment processing, were also used as regressors to reduce the motion related artifacts.

Before computing the regression analysis, the low-frequency confounding effects were removed using a high-pass filter with a 120-s cut-off period. Serial correlations among scans were also estimated with an autoregressive model (AR(1)) to remove the high-frequency noise that contaminated in the EPI time series. The regression coefficients for left/right hand grasping were computed for each individual using the fixed-effect model and then taken into the group analysis using a random-effect model of one sample *t*-test. The significant activation was decided by the height threshold at $p<0.0001$ (uncorrected for multiple comparison at the voxel level) and an extent threshold of 20 voxels. This combination of height and extent thresholds leads to a threshold at $p<0.001$ (corrected at the cluster level) in the current results.

Brain activities for the visually guided left/right hand-grasping task were identified by the voxel-based analysis of fMRI data (Fig. 2). Significant activations were found in the contra-lateral sensorimotor cortex, visual cortex, supplementary motor cortex, putamen (the activity extent to the thalamus), and secondary sensory cortex to the left/right grasped hand. The ipsilateral cerebellum also showed significant activation in association with hand grasping. The left premotor cortex was activated for both right and left hand grasping.

The voxels within a 10 mm radius sphere from the seed voxels of these regions were used as region of interests (ROIs) for identifying the EEG activity concerned with cortical activities. The coordinates of the seed voxels are shown in Table 1. The BOLD time series of all voxels within ROIs were averaged using Marsbar software (URL: marsbar.sourceforge.net). The averaged BOLD time series for ROIs were then detrended and band-pass filtered with 120 s to 10 s cut-off periods.

Analysis of the time–frequency representation of EEG power

Since MR imaging and cardioballistic artifacts contaminated the EEG measurements, the averaged waveforms of the MR and cardioballistic artifacts were subtracted from the contaminated periods using Brain Vision Analyzer software (Brain Products, Germany) (Allen et al., 1998, 2000). Ocular artifacts in the EEG were then corrected using EEG analyzing software (Brain Vision Analyzer, Brain Products, Germany) (Gratton et al., 1983). Briefly, the ocular artifacts were removed by subtracting the voltages of the vertical EOG (VEOG) and horizontal EOG (HEOG) channels, multiplied by a channel-dependent correction factor calculated on the basis of linear regression of this correction. Here, VEOG and HEOG were computed by subtracting the EOG data from EEG at Fp1 and Fp2 electrodes. The reference of the ocular corrected EEG was then changed to the average of all scalp electrodes and down-sampled to 200 Hz. The preprocessed EEG data were exported to Matlab (Mathworks Inc., USA) software for further analyses.

The EEG data were transformed into time–frequency representations of EEG power from 2 Hz to 50 Hz in 30 logarithmically spaced steps, using the Morlet wavelet, which is defined by the following equation (Tallon-Baudry et al., 1997).

$$w(t,f) = \left(\sigma_t\sqrt{\pi}\right)^{-1/2} \exp\left(-t^2/2{\sigma_t}^2\right) \exp(i2\pi f t), \quad (1)$$

where t is time, f is frequency and σ_f is the variance at the frequency f. σ_f is expressed by σ_t, which is the variance at time t, as $\sigma_f = 1/(2\pi\sigma_t)$. The wavelet is characterized by the ratio of the frequency to the variance (f/σ_f) and was set to be $f/\sigma_f = 7$ in the current study. Convolving the mother wavelet expressed in Eq. (1) to the EEG time series $s_n(t)$

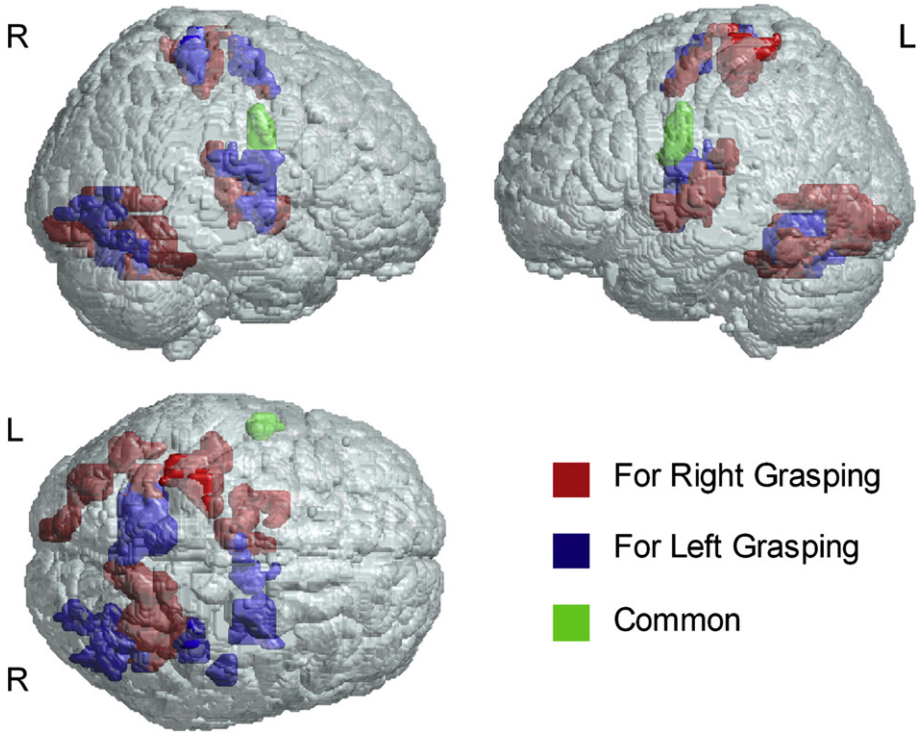

Fig. 2. The activations for right and left hand grasping are superimposed onto a glass brain. (Red) Activations for right hand grasping. (Blue) Activations for left hand grasping. (Green) Common activation for right and left hand grasping. Activations were identified by a height threshold at $p<0.0001$ (uncorrected for the multiple comparison) and an extent threshold of 20 voxels. R: right and L: left.

Table 1
fMRI results of anatomical regions, seed voxel coordinates (MNI), and *t*-value for the significant activations in association with left/right hand grasping.

Anatomical region	Brodmann area	MNI coordinates (mm)			*t*-Value
		x	y	z	
For right grasping					
L sensorimotor cortex	4/3	−39	−36	60	8.80
L visual cortex	19	−39	−84	−10	8.66
L supplementary motor cortex	6	−12	−15	65	6.05
L putamen/thalamus		−27	3	−5	6.44
L secondary sensory cortex	13	−48	−24	20	8.00
R cerebellum		24	−57	−20	9.66
L premotor cortex	6	−63	−6	35	9.21
For left grasping					
R sensorimotor cortex	4/3	36	−39	70	7.30
R visual cortex	19	42	−78	−10	6.65
R supplementary motor cortex	6	6	−12	65	7.27
R putamen/thalamus		24	−6	−5	7.86
R secondary sensory cortex	13	48	−21	15	6.65
L cerebellum		−15	−57	−15	10.52
L premotor cortex	6	−63	−6	35	5.92

Results are thresholded at $p<0.0001$ (uncorrected for the multiple comparison) and an extent threshold of 20 voxels, except for the premotor cortex for left hand grasping. The cluster size is 7 voxels in the premotor cortex for left hand grasping. MNI: Montreal Neurological Institute.

allowed the computation of the EEG power $e_n(t,f)$ at electrode n by the following equation:

$$e_n(t,f) = \log_{10}|w(t,f)\otimes s_n(t)|^2, \quad (2)$$

where ⊗ represents the convolution. The time–frequency representation of EEG power computed by Eq. (2) was used for further analyses.

Combined analyses of fMRI and EEG data

The scalp EEG power distribution that correlated with the cortical activity was identified by computing a forward model using multiple regression analysis between the time series of EEG power and the time series of cortical neuronal activities. The scalp-recorded EEG is the summation of the neuronal activities spatially distributed in the cortices (Fig. 1B). This spatial relationship was expressed by the forward model in the following equation:

$$e_n(t,f) = \boldsymbol{\beta}_n^{f\,\mathrm{T}}\mathbf{x} + \boldsymbol{\varepsilon}, \quad (3)$$

where $\mathbf{x}$ is the matrix of neuronal activities for fMRI ROIs in association with left/right hand grasping respectively; $\boldsymbol{\beta}_n^f$ is the regression coefficients vector for electrode n and frequency f; and $\boldsymbol{\varepsilon}$ is the residual vector. The regression coefficient β is a function of frequency (i.e., regression coefficients were computed for each frequency).

For EEG analysis, how a cortical activity contributes to the signals measured on the scalp is usually computed using complex realistic head models. The brain tissues (gray matter, white matter, skull, etc.) are electrically heterogeneous, and have different conductivities (Neilson et al., 2005). Thus, to arrive at an adequate estimation, the contribution to the scalp signals has to be computed by considering the brain structures and their electrical conductivity. On the other hand, if one can directly compare the scalp signal with the cortical neuronal activities, then how the cortical activity contributes to the scalp signal can be estimated by a direct comparison of these signals without considering the complex brain structure (Fig. 1B).

In the simultaneous fMRI and EEG, the cortical neuronal activities can be measured as BOLD responses. Both the scalp and cortical signals are observable in this measurement. Thus, the BOLD signal was used as the independent variable in Eq. (3) instead of the actual neuronal activity. Prior to computing Eq. (3), the mean of the BOLD time series was z-transformed to remove the risk of ill-conditioning, and to reduce the variance inflation in the coefficient estimates (Marquardt and Snee, 1975).

Note that the BOLD signal is a response to the neuronal activities with a time delay that is determined by the hemodynamic responses (Logothetis et al., 2001), while the dependent variable (i.e., the scalp EEG signal) is determined by electric neuronal activity. Many previous analyses on simultaneous fMRI and EEG have been concerned with the hemodynamic response in the computation of the EEG and BOLD relationship; this was in order to bridge this temporal gap between the BOLD and the neuronal activity (Goldman et al., 2002; Martinez-Montes et al., 2004; Moosmann et al., 2003). In line with these previous assumptions, the current study computed the convolution of the canonical hemodynamic response function and the EEG power time series to bridge the fMRI and EEG data, and then subsampled at the scan timing of the fMRI measurements. Before convolving the hemodynamic response function with it, the EEG power time series was detrended and z-transformed.

In a regression model, the predictors (i.e., the BOLD time series used for matrix $\mathbf{x}$ in Eq. (3)) should be independent variables for accurate computation of the correlation coefficients $\boldsymbol{\beta}_n^f$. The multicollinearity can be identified by the variance inflation factor (VIF) expressed by the following equation (Marquardt, 1970):

$$\mathrm{VIF}_i = 1/\left(1-R_i^2\right), \quad (4)$$

where R_i^2 is the multiple coefficient in a regression of the ith predictor on all other predictors. VIF_i is the variance inflation factor for ith predictor. If the ith predictor is completely independent from other predictors, the VIF becomes 1. If the maximum VIF becomes more than 10, it is judged as serious multicollinearity (Marquardt, 1970), and then the regression model expressed in Eq. (3) should not be applied.

In the computation of VIF for right hand grasping, one participant showed a maximum VIF > 10. This participant was excluded from the computation of the regression analysis. For left hand grasping, all VIFs were less than 10. The averages of VIFs among the participants were significantly less than 10 for both left and right hand grasping (Fig. 3). The independence of the predictor variables in the multiple regression analysis can be guaranteed by several methods that shrink the independent variables by a penalized regression analysis (e.g., ridge regression analysis). In the current study, one of the main objectives was to reconstruct the cortical EEG activities where the spatial location was decided by the fMRI analysis. Therefore, the VIF was used to guarantee the independency rather than using a shrink regression, which would have reduced the number of independent variables and lost the one-on-one relationship between the independent variable and cortical ROI. However, the VIF method may be too conservative, since data exceeding the VIF threshold

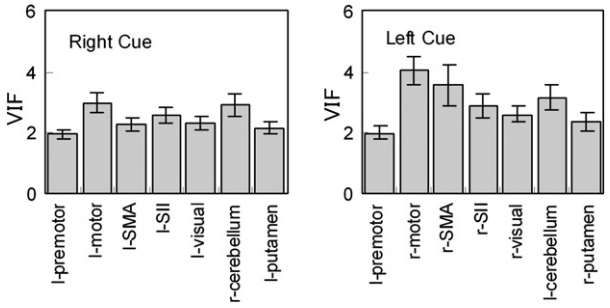

Fig. 3. Results of the variance inflation factor (VIF) among the BOLD signals in cortical ROIs. For the right cue, one participant was excluded from the analysis due to a high VIF (n = 13 for right cue, n = 14 for left cue).

were discarded from further analysis. This can be avoided by using a penalized regression analysis to determine the regression coefficients for multiple regression analysis.

The regression coefficient $\boldsymbol{\beta}_n^f$ of the forward model was computed for each participant with the least squares method and then taken into the group analysis using a random-effect model of one sample *t*-test. Significant correlation was decided by the bootstrap method (Efron, 1979; Efron and Tibshirani, 1986). The bootstrap procedure frees researchers from making unverifiable and most likely invalid assumptions about their data (e.g., probability distribution) prior to analysis (Di Nocera and Ferlazzo, 2000). This procedure is often used to handle correlations among statistical comparisons and to estimate empirical Type I error rate in electrophysiological measures (Di Nocera and Ferlazzo, 2000). In the bootstrap method, the individual zero-mean regression coefficient was randomly chosen 1000 times with allowing the duplication. The 1000 bootstrap resamples were tested with a one-sample *t*-test. The empirical distribution of *t*-value for the bootstrap resamples was then obtained. The bootstrap method was used for the correction against the multicollinearity caused by the inter-correlation of the analytic window in the wavelet analysis. The threshold based on empirical distribution indicated that a multiple comparison problem still remained. Therefore, the multiple comparison among the number of electrodes was corrected by the false discovery rate (FDR) and the probability in the empirical distribution computed by the bootstrap method was used for the FDR correction. In this study, the statistical threshold for the EEG topography decided by this procedure (FDR corrected $p<0.05$).

Reconstruction of cortical EEG power

In the reconstruction, the current study adopted the beamformer method (Herdman and Cheyne, 2009) which reconstructs the neuronal signal $s(t)$ at the spatial position r in the cortex using the equation: $\hat{s}_r(t) = \mathbf{w}^{\mathrm{T}}\mathbf{m}(t)$, where $\mathbf{m}$ represents the measured signal vector at the sensor (i.e., the EEG electrodes in the current study), and $\mathbf{w}$ is the beamformer spatial filter. The spatial filter $\mathbf{w}$ is estimated by a forward model that determines how a source at each point r would contribute to the signals $\mathbf{m}$ measured on scalp (Green and McDonald, 2009). The regression coefficient $\boldsymbol{\beta}_n^f$, which was computed by the multiple regression analysis between the EEG power time series and cortical neuronal activities, was used as the beamformer spatial filter $\mathbf{w}$. Thus, the EEG power $e_r(t)$ at frequency f and ROI r was reconstructed by the following equation:

$$\hat{e}_r^f(t) = \boldsymbol{\beta}_r^{f\mathrm{T}}\mathbf{e}^f(t), \tag{5}$$

where $\boldsymbol{\beta}_r$ is the regression coefficient vector containing the regression coefficients β_n for ROI r, and $\mathbf{e}(t)$ is the EEG power vector containing the EEG power $e_n(t)$. The EEG power time series was z-transformed before applying this method.

The temporal property of the cortical EEG power time series was analyzed for the contralateral/ipsilateral cortex to the grasped hand. Here, 'contralateral' refers to the ROIs identified by the left/right GO signal, where the activations were mostly found in the 'contralateral cortical hemisphere' to the hemifield of GO signal presentation. These were used to reconstruct the EEG power time series for the left/right GO signal presentation. In contrast, 'ipsilateral' refers to the ROIs identified by the right GO signal that were used to reconstruct the EEG power time series for the left GO signal presentation, and vice versa. In order to show the temporal property of the cortical EEG power time series, the following steps were performed in association with the onset of the informative cue and GO signal for hand grasping. The power ratio of individual reconstructed EEGs was computed by dividing by the grand median of the EEG power time series at each frequency, and then averaging across events within participants. The reconstructed EEGs were then averaged across participants, and compared between contralateral and ipsilateral conditions using a two-sample *t*-test. Correction against the multicollinearity of the wavelet analytic windows was made by choosing 5000 bootstrap resamples from the zero-mean translated data of the reconstructed EEG, and computing the *t*-statistical values by comparing contralateral and ipsilateral conditions. Based on this empirical distribution, the probability of the *t*-statistical values was computed for the power ratio modulation, and incorporated into the FDR correction.

Results

EEG topographical distribution of fMRI ROIs

The scalp EEG distribution associated with the cortical activities was identified by performing a multiple regression analysis between the EEG power time series and the BOLD signals in ROIs. For right hand grasping, EEG power (peak frequency = 11.8 Hz) at the left central electrodes was negatively correlated with the BOLD activity in the left sensorimotor cortex, and this activity corresponded with the mu rhythm (Fig. 4A). For left hand grasping, the EEG power of the mu rhythm at the contralateral electrode sites also showed a significant negative correlation with the right sensorimotor cortical activity (Fig. 4B). The gamma frequency oscillation (35.8 Hz) on the scalp electrode sites around the sensorimotor cortex indicated a significant positive correlation between the EEG power and the BOLD signal in the sensorimotor cortex. Note that the correlation of the gamma activity and the BOLD signal was positive, i.e., the EEG power was enhanced at the lateral-central sites when the BOLD signal increased in the right sensorimotor cortex (Fig. 4B).

A significant negative correlation was found between the EEG power and the BOLD time series at the alpha activity around the occipital electrode sites, in association with the activity in the visual cortex (10.6 Hz for left, and 9.5 Hz for right hemispheres; Fig. 5). The gamma activity also showed a significant correlation of the EEG power to the BOLD signal around the occipital electrode sites (35.8 Hz for left, and 44.7 Hz for right hemispheres; Fig. 5) in association with visual cortex activity. A negative correlation with EEG power was also found for the alpha activity around the central electrode sites with the BOLD activity in the supplementary motor cortex (8.5 Hz for right, and 9.5 Hz for left hand grasping; Fig. 6).

The locations of the electrodes that showed a significant correlation corresponded well geometrically with the location of the supplementary motor cortex. A positive correlation of the BOLD signal was found with the EEG power of gamma activity at the widely distributed scalp electrode sites in association with the left premotor cortex (35.8 Hz for right, and 32.1 Hz for left hand grasping, Fig. 7). No other activities found in the fMRI analysis showed a significant correlation of BOLD signals with the scalp EEG.

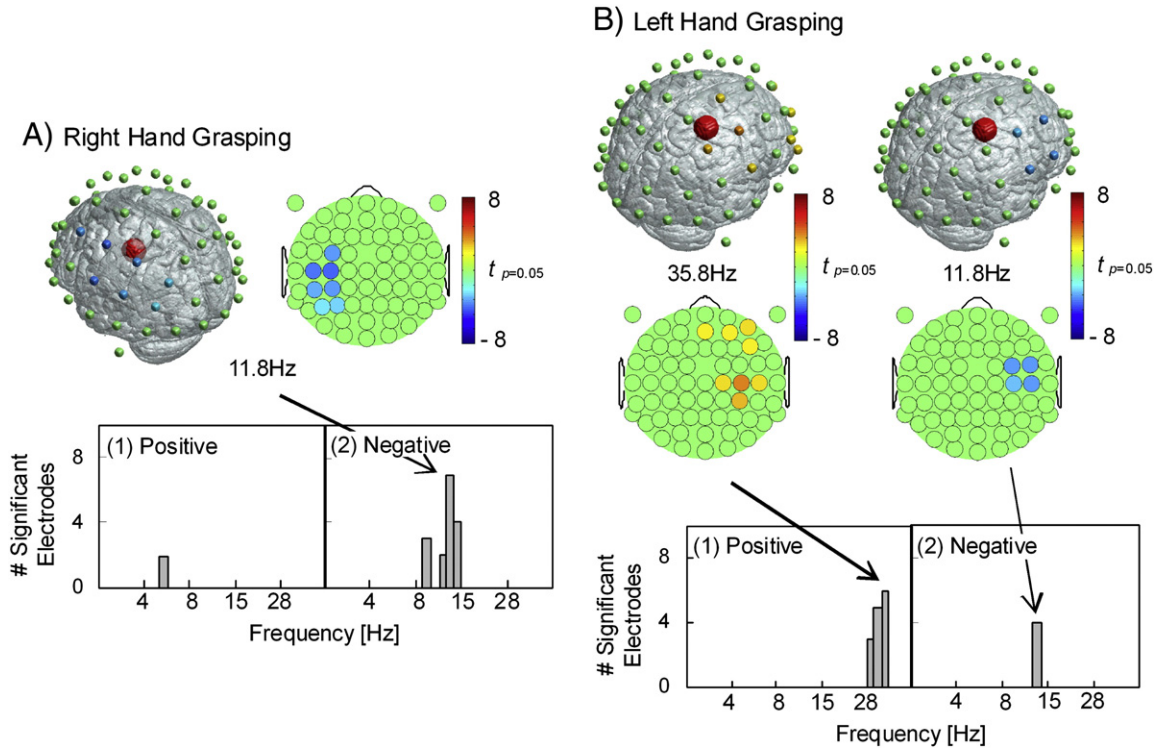

Fig. 4. Scalp EEG that correlates with the BOLD signal in the left sensorimotor cortex for right hand grasping (A) and in the right sensorimotor cortex for left hand grasping (B). (1) The histograms for the positive correlation of the BOLD and EEG power time series. (2) The histograms for the negative correlation of the BOLD and EEG power time series. These histograms show the numbers of electrodes that showed significant correlations (FDR corrected $p<0.05$). Consistent results for right and left hand grasping were found in the mu rhythm (peak of distribution is 11.8 Hz for right and left hand grasping) for the negative correlation. The gamma rhythm (35.8 Hz) was also found for the left hand grasping as the positive correlation (FDR corrected $p<0.05$). The topography shows the *t* statistical value of the correlation coefficients in the multiple regression analysis of BOLD signals to EEG power by a one-sample *t*-test at the peak frequency of distribution. The color bar represents the *t* statistical value. The fMRI ROI for the regression analysis is superimposed onto the glass brain. The electrode position is also superimposed around the glass brain, indicated as small spheres with colors corresponding to the topography.

Reconstruction of the cortical EEG power time series

The temporal profile of EEG activity was shown by reconstructing the cortical EEG power time series for the regions showing the significant temporal correlation of the BOLD signals in the ROIs to the scalp EEG power fluctuation (i.e., sensorimotor, visual, and supplementary motor cortices). The activity for the putamen, the secondary sensory cortex, and the cerebellum is not shown in this article, since no significant EEG activity was found on the scalp that correlated with the ROI BOLD signal. The dominant spatial position of the electrodes that showed the significant correlation of the EEG power to the BOLD signal in the premotor cortex was geometrically far from the location of the ROI of the premotor cortex. Hence, no conclusion can be made regarding the EEG activity in the right hemisphere as an indication of

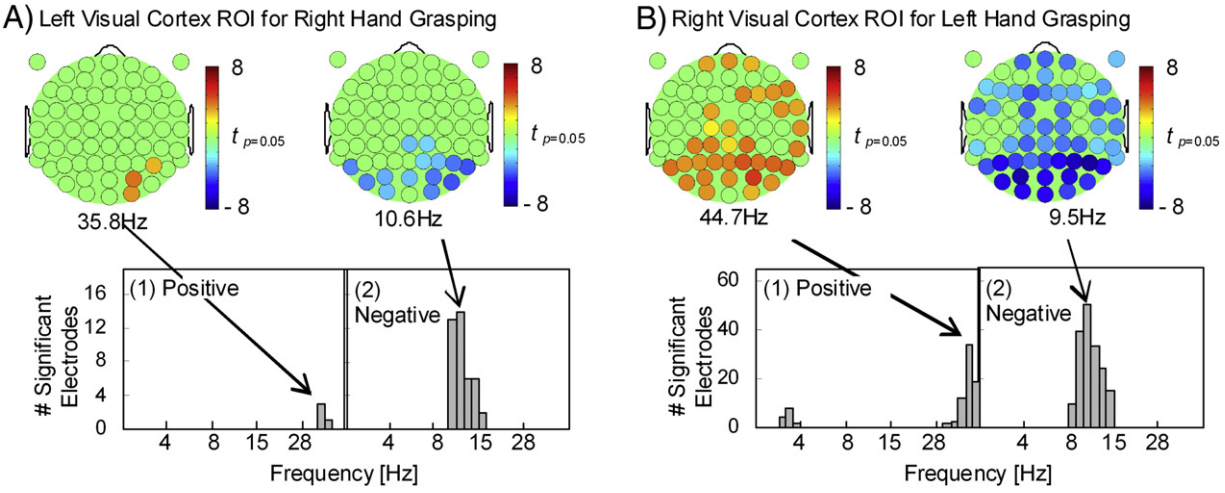

Fig. 5. Scalp EEG that correlated with the BOLD signal in the left visual cortex for right hand grasping (A) and in the right visual cortex for left hand grasping (B). (1) The histograms for the positive correlation of the BOLD and EEG power time series. (2) The histograms for the negative correlation of the BOLD and EEG power time series. These results show the numbers of electrodes that showed a significant correlation (FDR corrected $p<0.05$). Consistent results for right and left hand grasping were found in the gamma rhythm (peak of distribution is 35.8 Hz for right hand grasping, and 44.7 Hz for left hand grasping) for the positive correlation, and in the alpha rhythm (peak of distribution is 10.6 Hz for right hand grasping, and 9.5 Hz for left hand grasping) for the negative correlation.

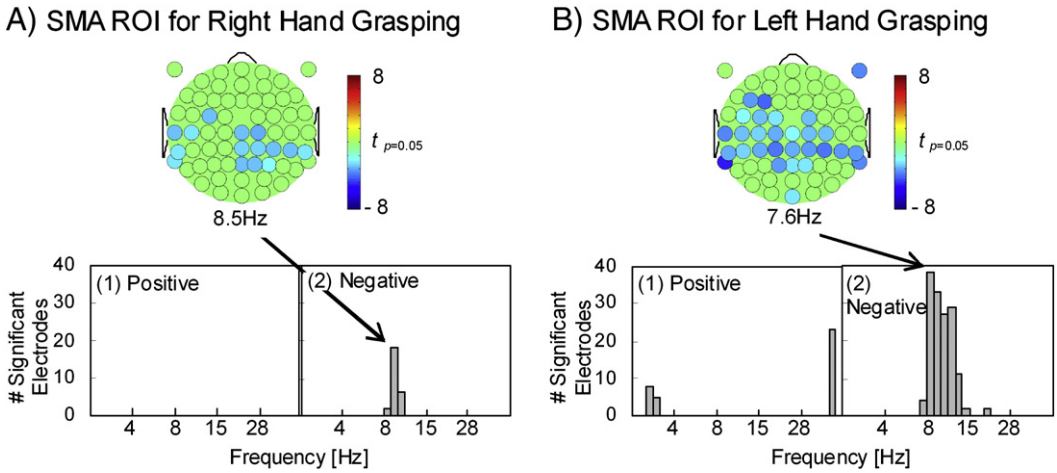

Fig. 6. Scalp EEG that correlated with the BOLD signal in the supplementary motor cortex for right hand grasping (A) and for left hand grasping (B). (1) The histograms for the positive correlation of the BOLD and EEG power time series. (2) The histograms for the negative correlation of the BOLD and EEG power time series. These histograms show the numbers of electrodes that showed significant correlation (FDR corrected $p<0.05$). Consistent results for right and left hand grasping were found in the alpha rhythm (peak of distribution is 8.5 Hz for right hand grasping and 7.6 Hz for left hand grasping) for the negative correlation. No consistent correlation for right and left hand grasping was found in the results of the positive correlation.

premotor cortical activity. The current reconstruction method was therefore not applied to the cortical EEG activity in the premotor cortex.

The mu rhythm of the reconstructed EEG power time series showed a suppression of EEG power after the informative cue presentation at the contralateral hemisphere to the sensorimotor cortices (around 10–16 Hz in Fig. 8). Note that the regression coefficients of mu rhythm for the sensorimotor cortex were negative (Fig. 4); thus, the positive value in the reconstructed results of the mu rhythm indicates a suppression of the EEG power, i.e., event related desynchronization. The suppression of mu rhythm in the sensorimotor cortex was sustained until the presentation of the GO signal (Fig. 10). After overshooting, the activity then returned to the baseline (Figs. 9 and 10). In addition to this mu suppression, a dominant modulation was also found around the delta/theta frequency band (2–8 Hz) that was associated with the informative cue and GO signal presentations. However, no significant correlation of the delta/theta EEG power to the BOLD was found for the left/right hand grasping conditions based on scalp topography (Fig. 4). Therefore, whether this activity represents an event-related synchronization or desynchronization is unclear.

Similar temporal profiles appeared for the alpha activities in the visual cortex and in the supplementary motor cortex. Since the alpha activities showed a negative correlation to the BOLD signals (Figs. 5 and 6), the increase in the reconstructed EEG activities around the alpha rhythm indicates a suppression of the EEG power. The alpha activities in the visual and supplementary motor cortices showed significant suppression of the EEG power after informative cue presentation for both the ipsilateral and contralateral conditions (Fig. 10A). Significant suppression of the alpha activities was also evident just before the GO signal presentation for the ipsilateral condition. These suppressions were sustained until the GO signal presentation, and then the values returned close to baseline after the overshoot (Fig. 10B). The lower frequency activities around the delta frequency band also showed the marked modulation associated with the GO signal presentation. In this case, again, whether these activities were the synchronization or desynchronization for the visual and supplementary motor cortices was unclear.

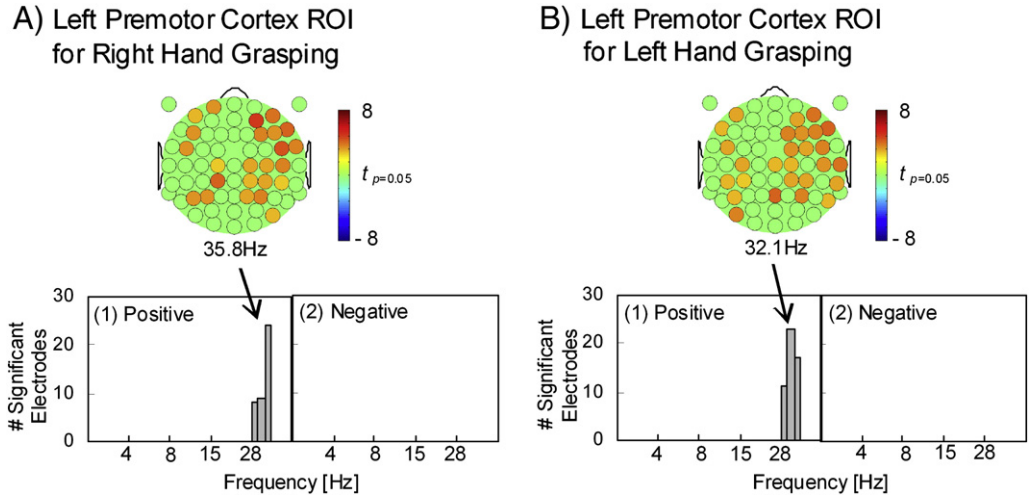

Fig. 7. Scalp EEG that correlated with the BOLD signal in the left premotor cortex for right hand grasping (A) and for left hand grasping (B). (1) The histograms for the positive correlation of the BOLD and EEG power time series. (2) The histograms for the negative correlation of the BOLD and EEG power time series. These histograms show the numbers of electrodes that showed a significant correlation (FDR corrected $p<0.05$). Consistent results for right and left hand grasping were found in the gamma rhythm (peak of distribution is 35.8 Hz for right hand grasping, and 32.1 Hz for left hand grasping) for the positive correlation. No consistent correlation for right and left hand grasping was found in the results of the negative correlation.

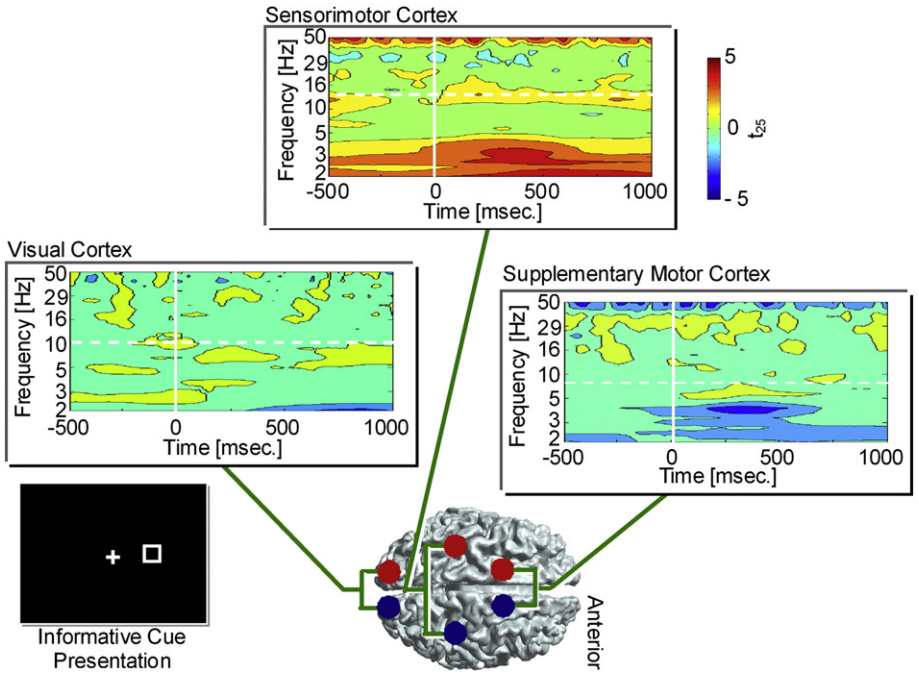

Fig. 8. Reconstructed cortical EEG power time series in association with the informative cue presentation. The EEG power time series was aligned to the onset of the informative cue presentation (t = 0 means the onset of informative cue presentation). The time–frequency representation shows the results of comparison of reconstructed cortical EEG power between 'contralateral' and 'ipsilateral' conditions by two-sampled *t*-test. Definitions of the 'contralateral' and 'ipsilateral' condition are described in the Materials and methods. Note that the positive *t* values represent the suppression of EEG power for the mu/alpha rhythms, since the regression coefficients of the mu/alpha rhythms were negative values in the regression analysis.

Discussion

EEG rhythms in the sensorimotor cortex

Previous studies considered the mu rhythm to represent an index of the activity in the sensorimotor cortex (Pfurtscheller et al., 1997; Tiihonen et al., 1989). In the sensorimotor cortex, the mu rhythm could be observed by direct recording of local field potential using electrocorticography (ECoG) (Pfurtscheller et al., 2003). However, few previous studies have reported concrete evidence for the origin of the scalp EEG mu rhythm, because of the difficulty in directly comparing scalp EEG and activity in the cortices. The present results show that the mu rhythm observed around the lateral central electrode sites, above the sensorimotor cortex, was significantly correlated with the actual activity in

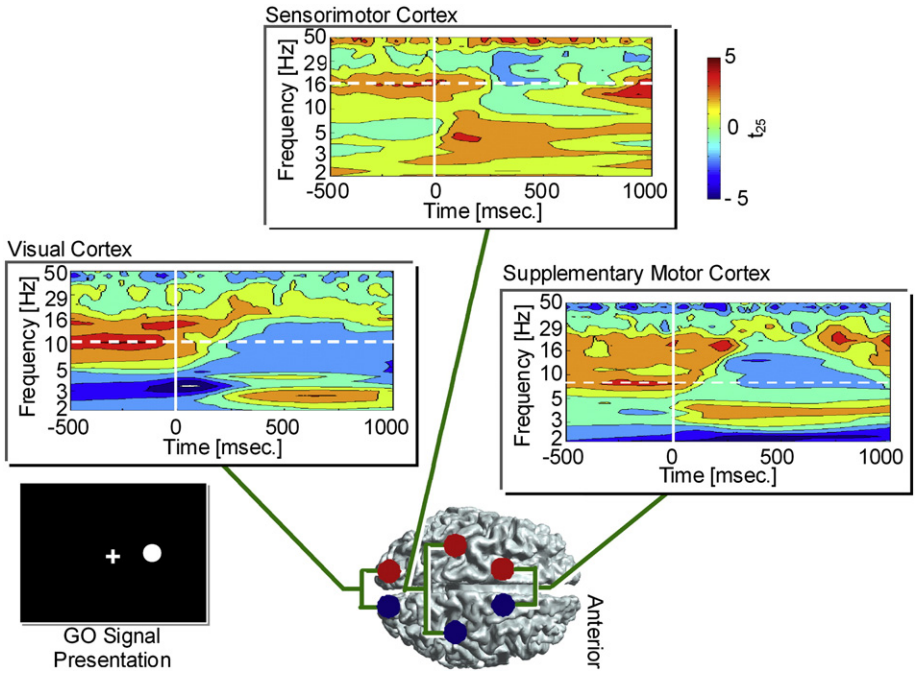

Fig. 9. Reconstructed cortical EEG power time series in association with the GO signal presentation. The EEG power time series was aligned to the onset of the GO signal presentation (*t* = 0 indicates the onset of GO signal presentation). The time–frequency representation shows the results of comparison of reconstructed cortical EEG power between 'contralateral' and 'ipsilateral' conditions by a two-sampled *t*-test.

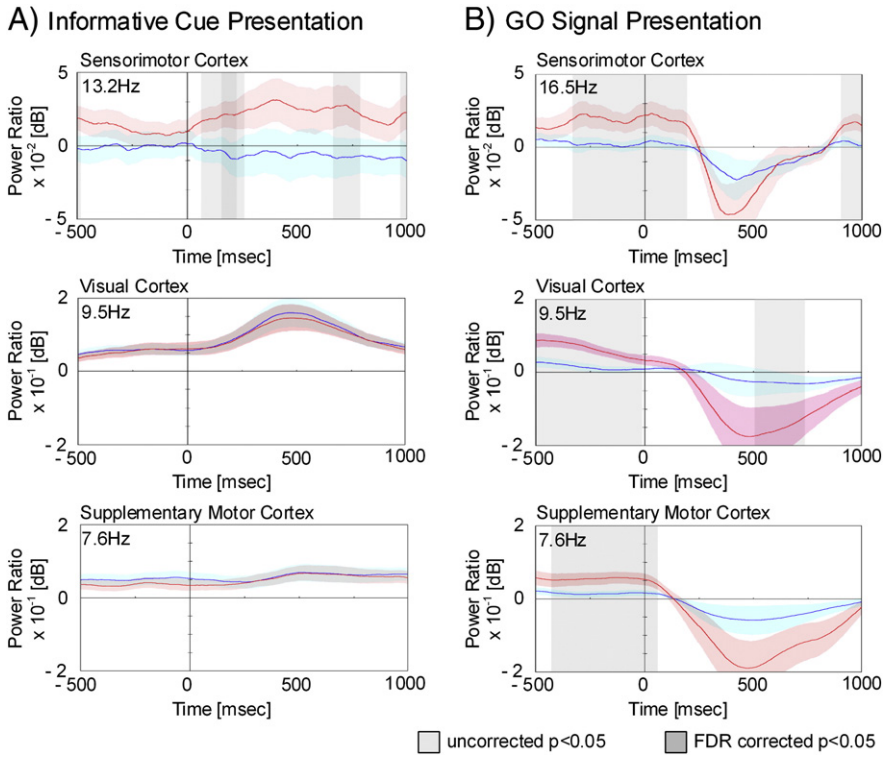

Fig. 10. The time series of reconstructed cortical EEG. (A) The power ratio of the reconstructed cortical EEG in association with the informative cue presentation. The red line and the red shaded area represent the mean power ratio and its standard error among participants for the 'contralateral' conditions. The blue line and blue shaded area are for the 'ipsilateral' condition. The darker gray shaded area represents the significant difference of the reconstructed cortical EEG between 'contralateral' and 'ipsilateral' conditions with the FDR correction for the multiple comparison for frequency and time analytic steps (FDR $p<0.05$). The light gray area represents the significant difference of the reconstructed EEGs without correction for the multiple comparison ($p<0.05$ uncorrected for the multiple comparison among time–frequency analytic steps). The frequencies for these results are shown as dashed lines in Figs. 8 and 9.

the sensorimotor cortex, as determined by direct comparison of neuronal activity (i.e., scalp EEG and BOLD) (Fig. 4). A temporal profile of the mu rhythm in the sensorimotor cortex was also evident following reconstruction of the EEG power time series in the cortex (Figs. 8–10).

This cortical mu rhythm showed suppression of activity after the informative cue presentation, and this suppression was sustained until the actual motor execution, after the GO signal presentation. Similar suppression was also reported in previous studies that used scalp EEGs, ECoGs, or magnetoencephalograms (MEGs). For example, Pfurtscheller et al. (2003) recorded the ECoG from the vicinity of the sensorimotor cortex during a palm pinch task, and identified the temporal profile of the mu rhythm. The mu rhythm was suppressed after the presentation of a GO signal to pinch the palm, in agreement with the current results. In contrast, the peak frequency of the mu rhythm was slightly higher than that observed in the current study for the correlation results on the scalp topography (Fig. 4).

The motor cortex of nonhuman primates shows a well-known beta rhythm, the dominant LFP pattern (Donoghue et al., 1998; Sanes and Donoghue, 1993; Spinks et al., 2008). This beta rhythm is specifically attenuated during movements related to reaching behaviors when compared to rhythms seen during instruction or post-movement periods (Donoghue et al., 1998; Spinks et al., 2008). The beta rhythm also shows selectivity with respect to reaching direction during the observation or hold periods (Spinks et al., 2008). In humans, the field potential measured by scalp recording (i.e., EEG) and LFP are synonymous terms, wherein both neurons and glia, and even blood vessels, can contribute to the mean field measured by the EEG (Buzsáki, 2006).

Human scalp EEG measurements show a similar temporal pattern to the beta rhythm seen in nonhuman primates (Pfurtscheller et al., 1997; Tiihonen et al., 1989; Wolpaw et al., 2002); i.e., the human motor cortex (Pfurtscheller et al., 2003) often shows a mu rhythm around the sensorimotor cortex. The reconstructed mu rhythm found in the present study in the sensorimotor cortex had a slightly higher frequency than that observed on the scalp (Figs. 8 and 9). Thus, the mu rhythm of scalp EEG measurements is analogous with the beta rhythm in the intracranial EEG measurements on the grounds of both functional and temporal profiles.

A simultaneous fMRI and EEG with a conventional method reported cortical areas that showed temporal correlation of the scalp EEG mu rhythm with the BOLD signal (Ritter et al., 2009). The study decomposed the scalp EEG activity using independent component analysis. The regression analysis was then computed using the EEG power time series of an independent component as a predictive variable. As in the present study, the origin of the mu rhythm was apparently in the sensorimotor cortex. The thalamus, cerebellum and many distributed cortices also had temporal correlations with the mu rhythm, although these regions were far from the electrode position where the mu rhythm was observed. This could have arisen due to the conventional use of scalp EEG activity as the independent variable in the regression analysis. The BOLD signals in these areas could have the correlation with BOLD in the sensorimotor cortex. On the other hand, the current method successfully showed that the mu rhythm originated in the sensorimotor cortex because the risk of a third-party effect had been reduced in the multiple regression analysis by using the cortical activities as the independent variables.

The scalp EEG is the summation of the multiple neuronal activities; consequently, EEG power bands might not always show the same inter-correlation. The skull's low-pass filter effect might depend on the frequency; therefore, the summation would also depend on the frequency. Furthermore, the width of the analytic temporal window in the wavelet transformation depends on the frequency. This causes quite different temporal profiles of the EEG power time series at each frequency. According to the above biological and analytical reasons, the regression coefficient was computed for each frequency in the current

study. However, the proposed method potentially includes a risk of ill-conditioning on the inter-frequency correlation. Some EEG power shows inter-frequency correlations (Scheeringa et al., 2011). In the conventional analysis for the simultaneous fMRI and EEG, the EEG power time series for multiple frequency bands were sometimes used as the independent variables in the multiple regression analysis. The simultaneous inclusion of the multiple-frequency bands in the independent variables can reduce the risk of the third-party effect caused by the inter-frequency correlation of the EEG power time series. On the other hand, in the current study, the EEG power time series were used as dependent variables.

The same strategy as the conventional method cannot be applied to the proposed method to reduce the risk. If the alpha/mu and gamma activities (those that had shown correlation with the cortical activities in the current results) had the inter-correlation, then the alpha/mu or gamma EEG activity may have falsely shown a correlation with the cortical activity. In fact, the gamma EEG was independent from the temporal fluctuation of the alpha and beta EEG power, while the alpha and beta EEG activities showed a strong temporal correlation with each other (Scheeringa et al., 2011).

In the current results, only the alpha/mu and gamma EEG activities showed significant correlation with the cortical activities. No duplicate activities were found in the alpha and beta EEG frequencies. The results of the alpha/mu and gamma activities would be the true correlation with the cortical activities—but not the artifactual correlation caused by the inter-frequency correlation of the EEG signal. However, the risk of inter-frequency correlation may still remain in the proposed method. To reduce the risk of artifactual results caused by the inter-frequency correlation, some factor analyses (e.g., independent component analysis) can be used to decompose the EEG activities into independent components prior to applying the proposed method. It would be a further step to improving the proposed method.

Nevertheless, a risk still remains that the scalp EEG does not represent the cortical neuronal activity seen at the fMRI ROIs. These ROIs that were used for the reconstruction of EEG are just the tip of the iceberg when considering the real neuronal activity and do not represent the total neuronal activity. Multiple regression analysis in this case might fail to rule out contamination from the cortical region, which would not be detected by conventional fMRI analysis. The risk also exists for a nonlinear relationship between the scalp EEG activity and fMRI BOLD signals due to non-neurophysiological artifacts. Therefore, the true origin may not be correctly identified, leading to inappropriate reconstruction of the cortical EEG activity.

Gamma activity was also identified in association with the activity in the sensorimotor cortex (Fig. 4B). Gamma activity and the beta rhythm are considered to represent different sub-functions in motor execution (Engel and Fries, 2010). The beta rhythm is tightly coupled to the maintenance of the motor state; e.g., holding something. The suppression of the beta rhythm then occurs when some motor command to change the motor state arises from the sensorimotor cortex. The gamma activity, on the other hand, is more concerned with the motor command itself. As discussed above, the mu rhythm in the scalp EEG could be synonymous with the beta rhythm in the intracranial EEG. Therefore, in the current study, the gamma activity, rather than the mu rhythm, might be enhanced after an informative cue presentation as a way of preparing for motor execution.

Alpha rhythm in associated cortices

Other correlations were evident between the scalp EEG and cortical activities in the supplementary motor cortex and in the visual cortex. These cortices also showed negative correlations with the EEG power in the alpha frequency range (Figs. 5 and 6). A significant correlation appeared in the topography at scalp electrode sites just around the supplementary motor cortex or visual cortex. The alpha activity occurring around the occipital electrode sites is also known as the resting alpha activity. Previous studies of simultaneous EEG and fMRI or positron emission tomography (PET) reported that the alpha activity at these sites is correlated with the suppression of the hemodynamic responses in the visual cortex (Goldman et al., 2002; Martinez-Montes et al., 2004; Sadato et al., 1998). These previous studies identified the origin of the alpha activity as well as other correlated cortices, since the hemodynamic responses in the other cortices (e.g., frontal cortex or thalamus) also showed significant correlation with the temporal fluctuation of alpha EEG power. This correlation was due to the direction of the analysis to bridge the hemodynamic measures and the EEG activity; i.e., the scalp EEG activity was used as the explanatory variable for regression analysis.

Correlational networks, or so-called functional connectivity networks, are known to exist in the cortex as a default mode network (Power et al., 2010; Raichle et al., 2001). Therefore, these previous studies might have introduced artifactual cortical activities that were correlated with the generator of the scalp EEG, even though not the true origin of the scalp EEG activity. The approach taken in the current study would reduce the risk of introducing this type of false positive activity by using the BOLD time series rather than the scalp EEG power as the explanatory variable to show the correlation to the EEG power, thereby reducing contamination from other cortical activities.

A similar temporal pattern to the alpha activity in the visual cortex was also found for the alpha activity in the supplementary motor cortex (Figs. 8–10). The task in the present study involved the participants grasping their left/right hands in accordance with the visual cue. The supplementary motor cortex is crucial for the selection of the left/right hand for motor execution (Hoshi and Tanji, 2004). The use of an informative cue presentation prior to the actual motor execution for hand grasping forced the participants to decide which hand should grasp after the GO signal presentation. Therefore, the alpha activity showed modulation after the informative cue presentation, and this activity could reflect the selection of the left/right hand for motor execution.

Positive and negative BOLD correlation

Both positive and negative correlations appeared between the EEG power and the BOLD time series. The fMRI BOLD signals are known to correlate more strongly with the LFP rather than with spike activity. A simultaneous measurement of fMRI and LFP in the nonhuman primate visual cortex showed an enhancement of gamma rhythm that was tightly coupled with a BOLD signal increase (Logothetis et al., 2001). This positive correlation between the LFP gamma activity and the hemodynamic activity was also shown by simultaneous recording of LFP and the optical imaging in the feline visual cortex (Niessing et al., 2005). The present results showing a positive correlation between the BOLD signal in the visual cortex and the gamma EEG power around the scalp occipital sites (Fig. 5) are consistent with these previous findings. This relationship was expected in the human brain, based on separate scalp EEG and fMRI measurements reported in a previous study (Martuzzi et al., 2009). A similar relationship between the scalp EEG power of gamma rhythm and the fMRI BOLD was also found in the visual cortex in a study on simultaneous fMRI and EEG (Scheeringa et al., 2011).

The gamma activity of the scalp EEG has been reported as merely reflecting an artifact caused by the micro-saccadic eye movement (Yuval-Greenberg et al., 2008). Micro-saccadic artifacts commonly show a broadband gamma activity up to 100 Hz. Confirmation of gamma activity as an artifact might be possible by analyzing the EEG spectrum up to 100 Hz. However, the signal to noise ratio at high frequency is reduced for EEG data simultaneously measured with fMRI. For this reason, the EEG power spectrum was analyzed up to 50 Hz in the current study. The EEG spectrum analysis could not eliminate the possibility of contamination of micro-saccadic artifacts on the gamma band activity in the current study.

Micro-saccadic artifacts have been known to appear around the ocular electrode when the average of all electrodes is used as the reference. Topographic mapping of EEGs by the commonly used Laplace operator could also induce a gamma band artifact on the scalp, when one discards EOG data during computation of the scalp EEG distribution (Keren et al., 2010). The averaging reference was used in the present study to show the EEG topography without the Laplace operator. The statistical results at the exact electrode positions are shown in Figs. 4–7, with the results for the EOG electrodes. Therefore, the current results are clearly far removed from the scenario of micro-saccadic artifacts. The gamma band activity reported here is therefore more likely to have reflected the true cortical activity. Note, however, that the gamma band activity showed no clear modulation in the reconstructed cortical EEG data in association with the informative cue and GO signal presentations. Therefore, the association of gamma band activity in the cortices is still questionable.

The alpha activity around the scalp occipital sites also showed a correlation with the BOLD in the visual cortex (Fig. 5). Notably, the regression coefficient falls into the negative value in this correlation; i.e., the alpha EEG power increased when the BOLD signal decreased. This negative correlation has also often been reported in previous studies that used simultaneous recordings of scalp EEG and various hemodynamic measures (Goldman et al., 2002; Moosmann et al., 2003; Sadato et al., 1998). In the present study, the BOLD signals in the sensorimotor cortex and the supplementary motor cortex also showed negative correlations with the cortical EEG power of the mu and alpha rhythms (Figs. 4 and 6).

Simultaneous fMRI and EEG measurements can provide additional information on the neuronal candidates involved in cognitive function via knowledge of the neurovascular coupling. Some researchers have assumed that a decrease in the hemodynamic response is associated with decreased spiking activity (Boorman et al., 2010; Shmuel et al., 2002). A negative correlation between spike rate and LFP power of the beta rhythm was reported in the motor cortex of nonhuman primates (Spinks et al., 2008). On the other hand, simultaneous recording of the LFP and optical imaging suggested that the lower frequency oscillation was negatively correlated with the hemodynamic response (Martuzzi et al., 2009).

Changing the time constant of the $GABA_A$-receptor-mediated GABA response is known to affect the frequency of the interneuron network oscillator (Buzsáki, 2006). Some cortical GABA interneurons cause arteriolar vasoconstriction; i.e., they decrease blood oxygenation levels in association with inhibitory synaptic activity (Devor et al., 2007). Taken together, the results showing a negative correlation between the BOLD signals and the mu/alpha rhythms would suggest involvement of the inhibitory synaptic activity among these cortical areas, whereas it might also indicate a correlation with a decrease in the firing rate because of the negative correlation of the LFP and the firing rate in the sensorimotor cortex.

In conclusion, a method is proposed for simultaneous recording of fMRIs and EEGs. This method can identify the scalp EEG distribution using the spatio-temporal information of the cortical activities measured by the fMRI. The activity in the sensorimotor cortex is associated with the mu rhythm recorded at the lateral central electrode sites, which demonstrates that the origin of the mu rhythm in the scalp EEG recording is in the sensorimotor cortex. Direct evidence is also presented for the existence of alpha rhythms in the occipital and supplementary motor cortices. The cortical EEG activity is reconstructed in a similar manner to the beamformer method used in the MEG (Green and McDonald, 2009; Herdman and Cheyne, 2009), but with the additional novelty of simultaneous fMRI and EEG measurements. The results allowed identification of the dynamics of cortical activity with the high temporal precision of EEG and the spatial precision of fMRI. The proposed method also can provide crucial information on the involvement of specific types of neurons (i.e., the excitatory or inhibitory neurons) based on neurovascular coupling. This new ability will allow better monitoring of human cortical dynamics in order to establish the underlying mechanism of neuronal computation for cognitive function.

Acknowledgment

The author expresses his appreciation to Dr. S. Takano and Mr. I. Fujimoto at ATR-Promotions, Japan for their technical support in performing the simultaneous fMRI and EEG measurements. He also expresses his gratitude to Prof. T. Inui for his comments on the early manuscript. This work was supported in part by a Grant-in-Aid for Scientific Research on Innovative Areas "Neural creativity for communication (No. 4103)" (21120008), a Grant-in-Aid for Young Scientists (A) (21680024), a Grant-in-Aid for Scientific Research (S) (20220003) of MEXT, and Mitsubishi Foundation.

References

Allen, P.J., Polizzi, G., Krakow, K., Fish, D.R., Lemieux, L., 1998. Identification of EEG events in the MR scanner: the problem of pulse artifact and a method for its subtraction. Neuroimage 8, 229–239.
Allen, P.J., Josephs, O., Turner, R., 2000. A method for removing imaging artifact from continuous EEG and recorded during functional MRI. Neuroimage 12, 230–239.
Boorman, L., Kennerley, A.J., Johnston, D., Jones, M., Zheng, Y., et al., 2010. Negative blood oxygen level dependence in the rat:a model for investigating the role of suppression in neurovascular coupling. J. Neurosci. 30, 4285–4294.
Buzsáki, G., 2006. Diversity of cortical functions is provided by inhibition & Windows of the brain. Rhythms of the Brain. Oxford Univ. Press, pp. 61–110.
Devor, A., Tian, P., Nishimura, N., Teng, I.C., Hillman, E.M., et al., 2007. Suppressed neuronal activity and concurrent arteriolar vasoconstriction may explain negative blood oxygenation level-dependent signal. J. Neurosci. 27, 4452–4459.
Di Nocera, F., Ferlazzo, F., 2000. Resampling approach to statistical inference: bootstrapping from event-related potentials data. Behav. Res. Methods Instrum. Comput. 32, 111–119.
Donoghue, J.P., Sanes, J.N., Hatsopoulos, N.G., Gaal, G., 1998. Neural discharge and local field potential oscillations in primate motor cortex during voluntary movements. J. Neurophysiol. 79, 159–173.
Dumas, G., Nadel, J., Soussignan, R., Martinerie, J., Garnero, L., 2010. Inter-brain synchronization during social interaction. PLoS One 5, e12166.
Efron, B.B., 1979. Bootstrap methods: another look at the Jackknife. Ann. Stat. 7, 1–26.
Efron, B.B., Tibshirani, R., 1986. Bootstrap methods for standard errors, confidence intervals, and other measures of statistical accuracy. Stat. Sci. 1, 54–77.
Engel, A.K., Fries, P., 2010. Beta-band oscillations—signalling the status quo? Curr. Opin. Neurobiol. 20, 156–165.
Goldman, R.I., Stern, J.M., Engel Jr., J., Cohen, M.S., 2002. Simultaneous EEG and fMRI of the alpha rhythm. Neuroreport 13, 2487–2492.
Gratton, G., Coles, M.G., Donchin, E., 1983. A new method for off-line removal of ocular artifact. Electroencephalogr. Clin. Neurophysiol. 55, 468–484.
Green, J.J., McDonald, J.J., 2009. A practical guide to beamformer source reconstruction for EEG. In: Handy, T.C. (Ed.), Brain Signal Analysis: Advance in Neuroelectric and Neuromagnetic Methods. MIT Press, pp. 79–98.
Herdman, A.T., Cheyne, D., 2009. A practical guide for MEG and beamforming. In: Handy, T.C. (Ed.), Brain Signal Analysis: Advance in Neuroelectric and Neuromagnetic Methods. MIT Press, pp. 99–140.
Hoshi, E., Tanji, J., 2004. Differential roles of neuronal activity in the supplementary and presupplementary motor areas: from information retrieval to motor planning and execution. J. Neurophysiol. 92, 3482–3499.
Keren, A.S., Yuval-Greenberg, S., Deouell, L.Y., 2010. Saccadic spike potentials in gamma-band EEG: characterization, detection and suppression. Neuroimage 49, 2248–2263.
Kiebel, S.J., Friston, K.J., 2004. Statistical parametric mapping for event-related potentials: I. Generic considerations. Neuroimage 22, 492–502.
Logothetis, N.K., Pauls, J., Augath, M., Trinath, T., Oeltermann, A., 2001. Neurophysiological investigation of the basis of the fMRI signal. Nature 412, 150–157.
Marquardt, D.W., 1970. Generalized inverses, ridge regression, biased linear estimation, and nonlinear estimation. Technometrics 12, 591–612.
Marquardt, D.W., Snee, R.D., 1975. Ridge regression in practice. Am. Stat. 29, 3–20.
Martinez-Montes, E., Valdes-Sosa, P.A., Miwakeichi, F., Goldman, R.I., Cohen, M.S., 2004. Concurrent EEG/fMRI analysis by multiway Partial Least Squares. Neuroimage 22, 1023–1034.
Martuzzi, R., Murray, M.M., Meuli, R.A., Thiran, J.P., Maeder, P.P., et al., 2009. Methods for determining frequency- and region-dependent relationships between estimated LFPs and BOLD responses in humans. J. Neurophysiol. 101, 491–502.
Miller, K.J., Leuthardt, E.C., Schalk, G., Rao, R.P., Anderson, N.R., et al., 2007. Spectral changes in cortical surface potentials during motor movement. J. Neurosci. 27, 2424–2432.
Millett, D., 2001. Hans Berger: from psychic energy to the EEG. Perspect. Biol. Med. 44, 522–542.
Mizuhara, H., Yamaguchi, Y., 2007. Human cortical circuits for central executive function emerge by theta phase synchronization. Neuroimage 36, 232–244.
Mizuhara, H., Wang, L.Q., Kobayashi, K., Yamaguchi, Y., 2004. A long-range cortical network emerging with theta oscillation in a mental task. Neuroreport 15, 1233–1238.
Mizuhara, H., Wang, L.Q., Kobayashi, K., Yamaguchi, Y., 2005. Long-range EEG phase synchronization during an arithmetic task indexes a coherent cortical network simultaneously measured by fMRI. Neuroimage 27, 553–563.
Moosmann, M., Ritter, P., Krastel, I., Brink, A., Thees, S., et al., 2003. Correlates of alpha rhythm in functional magnetic resonance imaging and near infrared spectroscopy. Neuroimage 20, 145–158.

Neilson, L.A., Kovalyov, M., Koles, Z.J., 2005. A computationally efficient method for accurately solving the EEG forward problem in a finely discretized head model. Clin. Neurophysiol. 116, 2302–2314.
Niessing, J., Ebisch, B., Schmidt, K.E., Niessing, M., Singer, W., et al., 2005. Hemodynamic signals correlate tightly with synchronized gamma oscillations. Science 309, 948–951.
Orgs, G., Dombrowski, J.H., Heil, M., Jansen-Osmann, P., 2008. Expertise in dance modulates alpha/beta event-related desynchronization during action observation. Eur. J. Neurosci. 27, 3380–3384.
Pfurtscheller, G., Neuper, C., Andrew, C., Edlinger, G., 1997. Foot and hand area mu rhythms. Int. J. Psychophysiol. 26, 121–135.
Pfurtscheller, G., Graimann, B., Huggins, J.E., Levine, S.P., Schuh, L.A., 2003. Spatiotemporal patterns of beta desynchronization and gamma synchronization in corticographic data during self-paced movement. Clin. Neurophysiol. 114, 1226–1236.
Power, J.D., Fair, D.A., Schlaggar, B.L., Petersen, S.E., 2010. The development of human functional brain networks. Neuron 67, 735–748.
Raichle, M.E., MacLeod, A.M., Snyder, A.Z., Powers, W.J., Gusnard, D.A., et al., 2001. A default mode of brain function. Proc. Natl. Acad. Sci. U.S.A. 98, 676–682.
Ritter, P., Moosmann, M., Villringer, A., 2009. Rolandic alpha and beta EEG rhythms' strengths are inversely related to fMRI-BOLD signal in primary somatosensory and motor cortex. Hum. Brain Mapp. 30, 1168–1187.
Sadato, N., Nakamura, S., Oohashi, T., Nishina, E., Fuwamoto, Y., et al., 1998. Neural networks for generation and suppression of alpha rhythm: a PET study. Neuroreport 9, 893–897.
Sanes, J.N., Donoghue, J.P., 1993. Oscillations in local field potentials of the primate motor cortex during voluntary movement. Proc. Natl. Acad. Sci. U.S.A. 90, 4470–4474.
Scheeringa, R., Fries, P., Petersson, K.M., Oostenveld, R., Grothe, I., Norris, D.G., Hagoort, P., Bastiaansen, M.C., 2011. Neuronal dynamics underlying high- and low-frequency EEG oscillations contribute independently to the human BOLD signal. Neuron 69, 572–583.
Shmuel, A., Yacoub, E., Pfeuffer, J., Van de Moortele, P.F., Adriany, G., et al., 2002. Sustained negative BOLD, blood flow and oxygen consumption response and its coupling to the positive response in the human brain. Neuron 36, 1195–1210.
Spinks, R.L., Kraskov, A., Brochier, T., Umilta, M.A., Lemon, R.N., 2008. Selectivity for grasp in local field potential and single neuron activity recorded simultaneously from M1 and F5 in the awake macaque monkey. J. Neurosci. 28, 10961–10971.
Tallon-Baudry, C., Bertrand, O., Delpuech, C., Permier, J., 1997. Oscillatory gamma-band (30–70 Hz) activity induced by a visual search task in humans. J. Neurosci. 17, 722–734.
Tiihonen, J., Kajola, M., Hari, R., 1989. Magnetic mu rhythm in man. Neuroscience 32, 793–800.
Ulloa, E.R., Pineda, J.A., 2007. Recognition of point-light biological motion: mu rhythms and mirror neuron activity. Behav. Brain Res. 183, 188–194.
Valdes-Sosa, P.A., Sanchez-Bornot, J.M., Sotero, R.C., Iturria-Medina, Y., Aleman-Gomez, Y., Bosch-Bayard, J., Carbonell, F., Ozaki, T., 2009. Model driven EEG/fMRI fusion of brain oscillations. Hum. Brain Mapp. 30, 2701–2721.
Wolpaw, J.R., Birbaumer, N., McFarland, D.J., Pfurtscheller, G., Vaughan, T.M., 2002. Brain–computer interfaces for communication and control. Clin. Neurophysiol. 113, 767–791.
Yuval-Greenberg, S., Tomer, O., Keren, A.S., Nelken, I., Deouell, L.Y., 2008. Transient induced gamma-band response in EEG as a manifestation of miniature saccades. Neuron 58, 429–441.